 CMC, vol.59, no.3, pp.1015-1026, 2019

Stability Analysis of Transfer Alignment Filter Based on the μ Theory

Lihua Zhu[1], Yu Wang[1], Lei Wang[2] and Zhiqiang Wu[1,*]

Abstract: The performance of the transfer alignment has great impact on inertial navigation systems. As the transfer alignment is generally implemented using a filter to compensate the errors, its accuracy, rapidity and anti-disturbance capability are key properties to evaluate the filtering process. In terms of the superiority in dealing with the noise, H∞ filtering has been used to improve the anti-disturbance capability of the transfer alignment. However, there is still a need to incorporate system uncertainty due to various dynamic conditions. Based on the structural value theory, a robustness stability analysis method has been proposed for the transfer alignment to evaluate the impact of uncertainty on the navigation system. The mathematical derivation has been elaborated in this paper, and the simulation has been carried out to verify the effectiveness of the algorithm.

Keywords: Robustness stability, transfer alignment, inertial navigation system, μ theory.

1 Introduction

In the recent literature, the issue of stability in various systems has received considerable attention. The transfer alignment of navigation system is one of the most popular methods for a moving base, which uses the observation difference between MINS (master inertial navigation system) and the SINS (slave inertial navigation system) to estimate the system errors by filters [Zhou, Lian, Yang et al. (2018)]. Similar to the most systems in use today, there are usually uncertainties incorporated in the navigation systems, which may model a number of factors, including: dynamics that are neglected to make the model tractable, as with large scale structures; nonlinearities that are either too hard or too complicated to model; and parameters that are not known exactly, either because they are hard to measure or there are varying manufacturing conditions [Candès, Romberg and Tao (2006)].

Since the H∞ performance is robust with respect to the input and observation noises, it has attracted much attention since the 1980s. The H∞ filtering is a state estimation of minimizing the maximum energy in the estimation error over all the disturbance trajectories [Yang and Che (2008)]. The state estimation based on this criterion is valid when a significant uncertainty exists in the disturbance statistics. Plus, the design for an H∞ filter does not require knowledge of the statistics of the system or the observation

[1] School of Mechanical Engineering, Nanjing University of Science and Technology, Nanjing, 210094, China.

[2] School of Computing and Information Technology, University of Wollongong, Northfields Ave, Wollongong NSW 2522, Australia.

[*] Corresponding Author: Wu Zhiqiang. Email: wuzhiqiang@njust.edu.cn.

noise and it possesses the robustness against the systems and noise uncertainties. To reduce the effect of the uncertainties on the system, H∞ filter has been applied to deal with the parameter uncertainties by increasing the robustness of the system [Zhao (2018); Wang and Yang (2018); Liu, Wang, He et al. (2017); Li, Chen, Zhou et al. (2009)].

The most general and accurate means of analyzing and characterizing the effect of system uncertainty on robust performance and stability, is the structured singular value μ-framework developed by Doyle and other researchers [Doyle (1985); Packard and Doyle (1993); Zhou, Doyle and Glover (1996)]. Allowing for the precise measurement of changing effects in operating conditions and uncertainty in model parameters on stability and performance robustness, this approach has been applied in various fields. For example, μ analysis was used to model the uncertainties and evaluate the stability of a power system [Liu (2018)]. Bottura et al. [Bottura and Neto (2000)] investigated μ-analysis to test robust stability and performance variations in speed control of an induction motor system. Zhao et al. [Zhao, Qiu and Feng (2016)] examined the robust stability of an integrated navigation system; He et al. [He, Wu and She (2004)] employed the μ analysis in exploring the robustness of the uncertain neutral systems with mixed delays. Pavel [Pavel (2004)] from University of Toronto had done research on stability of the optical communication networks with μ-analysis. Kim et al. [Kim and Cho (2016)] evaluated the robustness of a biochemical network through μ-analysis.

This paper presents an approach of robustness stability evaluation of transfer alignment for a moving base navigation system by using the structured singular value analysis(μ-analysis). It takes the input, the output, the transfer function, and the parameter variation into linear association and reconstruction, and then modifies the system to standard feedback system for the eventual analysis. This paper is organized as follows. Section 2 is devoted to introducing some basic notations and definitions of the structured singular value theory. Section 3 establishes the system model of the H∞ transfer alignment filter. After that, the derivation of alignment system model and uncertainty module with Linear fractional transformation (LFT) of feedback transfer alignment system is given in Section 4. Section 5 shows the simulation experiment with the proposed algorithm to test the validation of the algorithm. Concluding remarks are provided in Section 6.

2 Preliminary

Theoretically, the structured singular value is an extended concept of constant matrix singular value, which is also known as the m analysis. It is a powerful tool, to analyze the robust stability, nominal performance and the robust performance of dynamic systems.

The general feedback framework of m analysis with system $M(s)$ and the uncertainty $D(s)$ is shown in Fig. 1. Any linear interconnection of inputs, outputs and commands along with perturbations and controller can be viewed in this context and rearranged to match this diagram.

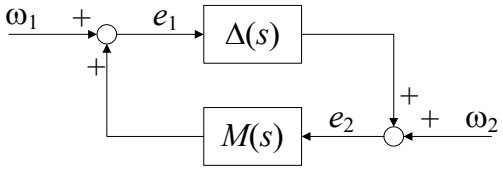

Figure 1: General feedback framework

Where, ω_1, ω_2 are the exogenous disturbing input vectors, e_1, e_2 are the error vectors. Given an uncertainty with known structure, bound value, the set $\boldsymbol{B\Delta}$, a set of possibly real and/or complex uncertainties.

$$\boldsymbol{\Delta}=\{diag(\delta_1 I_{r1},\ldots,\delta_S I_{rs},\Delta_1,\ldots\Delta_F),\delta_i\in C,\delta_j\in C^{m_j\times m_j}\} \tag{1}$$

$$\boldsymbol{B\Delta}=\{\Delta\in\boldsymbol{\Delta}|\,\bar{\sigma}(\Delta)\le 1\} \tag{2}$$

Where, $\bar{\sigma}(.)$ denotes the maximum singular value of a matrix and two non-negative integers S and F represent the number of repeated scalar blocks and full blocks, respectively. Consider the closed loop system with the constant matrix M(s) and the uncertainty Δ(s), the structured singular value $\mu_\Delta(M)$ is defined as:

$$\mu_\Delta(M):=\frac{1}{\min\{\bar{\sigma}(\Delta):\Delta\in\Delta,\det(I-M\Delta)=0\}} \tag{3}$$

In a word, the structured singular value is defined as the inverse of the smallest possible uncertainty.

The first step in the μ analysis is to derive a linear power converter model. The properties of μ, and the consequently the μ analysis results, refer to the LFT standard representation of the control problem. Linear fractional transformation is a matrix function, which is a useful way to standardize block diagrams for robust control analysis and design. Many control problems can be expressed within the framework of LFT, which is shown in Fig. 2 and Fig. 3. This framework can be used in describing and analyzing the uncertain system, where M is assumed to be the invariable part of the control system, while Δ is the block diagonal matrix. Then, the matrix M is partitioned as in Definition 1.

Definition 1 For a complex matrix M

$$M=\begin{bmatrix}M_{11} & M_{12}\\ M_{21} & M_{22}\end{bmatrix}\in \mathrm{C}^{(p_1+p_2)(q_1+q_2)} \tag{4}$$

And the complex matrices $\Delta_l=C^{q2\times p2}$ and $\Delta_u=C^{q1\times p1}$ of appropriate size define a lower LFT with respect to Δ_l as:

$$F_l(M,\Delta_l):=M_{11}+M_{12}\Delta_l(I-M_{22}\Delta_l)^{-1}M_{21} \tag{5}$$

Provided the inverse matrices $(I - M_{22}\Delta_l)^{-1}$ exists.

And an upper *LFT* with respect to Δ_u is defined as

$$F_u(M, \Delta_u) := M_{22} + M_{21}\Delta_u(I - M_{11}\Delta_u)^{-1}M_{12} \tag{6}$$

Provided the inverse matrices $(I - M_{11}\Delta_u)^{-1}$ exists.

$F_u(M, \Delta_u)$ and $F_l(M, \Delta_l)$ denote the upper LFT and the lower *LFT* separately, with the visual definition in Fig. 2 and Fig. 3, and the corresponding expressions are shown in Eqs. (7) and (8).

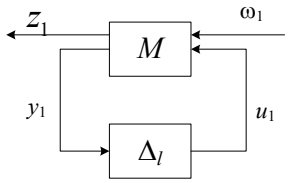

Figure 2: Lower LFT structure frame

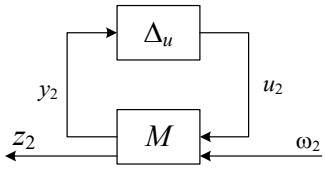

Figure 3: Upper LFT structure frame

Eq. (7) and Eq. (8) correspond to Fig. 2 and Fig. 3, respectively.

$$\begin{bmatrix} z_1 \\ y_1 \end{bmatrix} = M \begin{bmatrix} \omega_1 \\ u_1 \end{bmatrix} = \begin{bmatrix} M_{11} & M_{12} \\ M_{21} & M_{22} \end{bmatrix} \begin{bmatrix} \omega_1 \\ u_1 \end{bmatrix} \tag{7}$$

$$\begin{bmatrix} y_2 \\ z_2 \end{bmatrix} = M \begin{bmatrix} u_2 \\ \omega_2 \end{bmatrix} = \begin{bmatrix} M_{11} & M_{12} \\ M_{21} & M_{22} \end{bmatrix} \begin{bmatrix} u_2 \\ \omega_2 \end{bmatrix} \tag{8}$$

The explanation of *LFT* (take $F_l(M, \Delta)$ for example). A nominal mapping M_{11} is perturbed by uncertainty Δ, while M_{12}, M_{21} and M_{22} reflect how the uncertainty influences the nominal mapping.

Robust Stability Theorem: Assuming β>0, the closed-loop system in Fig. 1 is stable if and only if the condition in Eq. (9) is satisfied.

$$\sup_{\omega \in R} \mu_{\Delta}(G(j\omega)) \le \beta \tag{9}$$

For all Δ , such that $\Delta(\cdot) \in \mu(\Delta)$ while $\|\Delta\|_\infty < 1/\beta$

3 The system model of the filter

Unlike standard Kalman filter, there is no assumption on the statistical properties of the interference signal in H∞ filtering. Targeting at the systems with uncertainties and external interference, it is to build a filter that makes the H∞ norm of the filtering error output from the interference input minimized. The definition of the H∞ filter is:

Given γ>0，resolve the causality filter $F(s) \in RH_\infty$(if it exits)，make

$$J := \sup_{\omega \in L[0,\infty]} \frac{\| z - \hat{z} \|_2^2}{\| \omega \|_2^2} < \gamma^2 \tag{10}$$

Here, $\hat{z}=F(s)y$。

The transfer alignment system with the H∞ filter can be modeled by the following equations:

$$\begin{aligned} &\dot{\boldsymbol{x}}(k)=\boldsymbol{A}\boldsymbol{x}(k)+\boldsymbol{B}_1\boldsymbol{\omega}(k), \boldsymbol{x}(0)=0 \\ &\boldsymbol{z}(k)=\boldsymbol{C}_2\boldsymbol{x}(k)+\boldsymbol{D}_{21}\boldsymbol{v}(k) \\ &\boldsymbol{y}(k)=\boldsymbol{C}_1\boldsymbol{x}(k)+\boldsymbol{D}_{11} \end{aligned} \tag{11}$$

Fig. 4 shows the framework of the H∞ filter

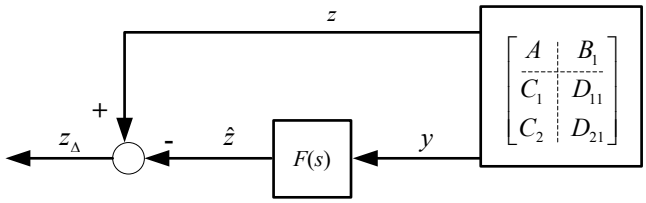

Figure 4: Framework of the H∞ filter

Where, $z_\Delta=z-\hat{z}$.

Using LFT to describe the H∞ filter, we could obtain the LFT of the H∞ filter.

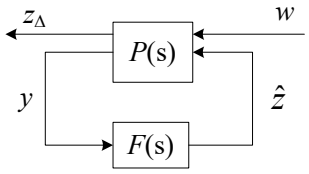

Figure 5: LFT description of the H∞ filter

Where, the system $P(s)$ shows as

$$P(s)=\begin{bmatrix} A & B_1 & 0 \\ C_1 & D_{11} & -I \\ C_2 & D_{21} & 0 \end{bmatrix} \tag{12}$$

Where, filter $F(s) \in RH_\infty$, and the Eq. (13) has to be satisfied for the H∞ filter.

$$\sup_{\omega \in L[0,\infty]} \frac{\| z_\Delta \|_2^2}{\| \omega \|_2^2} < \gamma^2 \tag{13}$$

According Fig. 5, Eq. (14) can be obtained as follows.

$$\hat{z} = F(s)y = \begin{bmatrix} A + L_{2\infty}C_2 + L_{1\infty}D_{112}C_2 & -L_{2\infty} - L_{1\infty}D_{112} \\ C_1 - D_{112}C_2 & D_{112} \end{bmatrix} y \tag{14}$$

Where,

$$\begin{bmatrix} L_{1\infty} & L_{2\infty} \end{bmatrix} = -\begin{bmatrix} B_1 D_{11}^T + Y_\infty C_1^T & B_1 D_{21}^T + Y_\infty C_2^T \end{bmatrix} \tilde{R}^{-1} \tag{15}$$

In our case $\boldsymbol{D}_{11}$=0 and $\boldsymbol{D}_{21}$=0， and the filter can be simplified as:

$$\hat{z} = \begin{bmatrix} A - Y_\infty C_2^T C_2 & Y_\infty C_2^T \\ C_1 & 0 \end{bmatrix} y \tag{16}$$

Where, $\boldsymbol{Y}_\infty$ is the positive definite solution of the equation in (17)

$$Y_\infty A^T + A Y_\infty + Y_\infty (\gamma^{-2} C_1^T C_1 - C_2^T C_2) Y_\infty + B_1 B_1^T = 0 \tag{17}$$

The system matrix $\boldsymbol{P}(s)$, the filter matrix $\boldsymbol{F}(s)$ can be divided into four blocks, as follows:

$$P(s) = \begin{bmatrix} A & \vdots & B_1 & 0 \\ \cdots & \cdots & \cdots & \cdots \\ C_1 & \vdots & D_{11} & -I \\ C_2 & \vdots & D_{21} & 0 \end{bmatrix}, \quad F(s) = \begin{bmatrix} A - Y_\infty C_2^T C_2 & Y_\infty C_2^T \\ C_1 & 0 \end{bmatrix}$$

Abbreviated as $P = \begin{bmatrix} P_{11} & P_{12} \\ P_{21} & P_{22} \end{bmatrix}$ and $F = \begin{bmatrix} F_{11} & F_{12} \\ F_{21} & F_{22} \end{bmatrix}$

So, P_{11}=A， $P_{12} = \begin{bmatrix} B_1 & 0 \end{bmatrix}$， $P_{21} = \begin{bmatrix} C_1 \\ C_2 \end{bmatrix}$， $P_{22} = \begin{bmatrix} 0 & -I \\ 0 & 0 \end{bmatrix}$

$\boldsymbol{F}_{11}$=$\boldsymbol{A}$-$\boldsymbol{Y}_\infty \boldsymbol{C}_2^T \boldsymbol{C}_2$, $\boldsymbol{F}_{12}$=$\boldsymbol{Y}_\infty \boldsymbol{C}_2^T$, $\boldsymbol{F}_{21}$=$\boldsymbol{C}_1$, $\boldsymbol{F}_{22}$=0

4 Robust stability analysis

According to the lower LFT, the transfer alignment system and the filter can be integrated into one representation $\boldsymbol{M}$, as shown in Eq. (18) below:

$$\boldsymbol{M}=\boldsymbol{P}_{11}+\boldsymbol{P}_{12}\boldsymbol{F}(\boldsymbol{I}-\boldsymbol{P}_{22}\boldsymbol{F})^{-1}\boldsymbol{P}_{21} \tag{18}$$

Applying the system model to Eq. (18), the following results can be obtained:

$$M = A + \begin{bmatrix} B_1 & 0 \end{bmatrix} \begin{bmatrix} F_{11} & F_{12} \\ F_{21} & F_{22} \end{bmatrix} (I - \begin{bmatrix} D_{11} & -I \\ D_{21} & 0 \end{bmatrix} \begin{bmatrix} F_{11} & F_{12} \\ F_{21} & F_{22} \end{bmatrix})^{-1} \begin{bmatrix} C_1 \\ C_2 \end{bmatrix}$$

$$= A + \begin{bmatrix} B_1 F_{11} & B_1 F_{12} \end{bmatrix} (I - \begin{bmatrix} D_{11}F_{11} - F_{21} & D_{11}F_{12} - F_{22} \\ D_{21}F_{11} & D_{21}F_{12} \end{bmatrix})^{-1} \begin{bmatrix} C_1 \\ C_2 \end{bmatrix} \quad (19)$$

$D_{11}=0$, $D_{21}=0$, $F_{21}=C_1=I$, $F_{22}=0$

$$\therefore M = A + \begin{bmatrix} B_1 F_{11} & B_1 F_{12} \end{bmatrix} (I - \begin{bmatrix} -F_{21} & -F_{22} \\ 0 & 0 \end{bmatrix})^{-1} \begin{bmatrix} C_1 \\ C_2 \end{bmatrix}$$

$$= A + \begin{bmatrix} \frac{1}{2} B_1 F_{11} & B_1 F_{12} \end{bmatrix} \begin{bmatrix} C_1 \\ C_2 \end{bmatrix} = A + \frac{1}{2} B_1 F_{11} C_1 + B_1 F_{12} C_2 \quad (20)$$

$$\because F_{11} = A - Y_\infty C_2^T C_2, \quad F_{12} = Y_\infty C_2^T, \quad C_1 = I$$

$$\therefore M = A + \frac{1}{2} B_1 (A - Y_\infty C_2^T C_2) C_1 + B_1 Y_\infty C_2^T C_2 = A + \frac{1}{2} B_1 A - \frac{1}{2} B_1 Y_\infty C_2^T C_2 + B_1 Y_\infty C_2^T C_2$$

$$= (\frac{1}{2} B_1 + I) A + \frac{1}{2} B_1 Y_\infty C_2^T C_2 \quad (21)$$

In order to extract the structural perturbation and introduce it into the feedback system, it is necessary to apply a series of transformations to *M*. Firstly, it is converted into the form of a feedback form shown in Fig. 6.

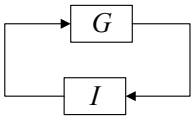

Figure 6: Standard feedback structure

Assuming that $\boldsymbol{G}$ contains structural perturbation $\boldsymbol{\Delta G}$, $\boldsymbol{G}=\boldsymbol{G}_0+\boldsymbol{\Delta G}$, where $\boldsymbol{G}_0$ is the nominal system without structural perturbation. The extracted perturbation $\boldsymbol{\Delta G}$ is then introduced to the feedback structure to do the robust analysis, shown in Fig. 7

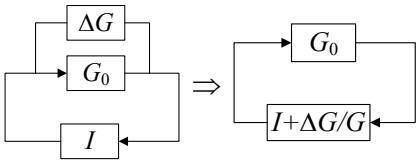

Figure 7: The feedback system with structural perturbation

$\boldsymbol{\Delta G}$ is generated by the structure disturbance $\boldsymbol{\Delta M}$ of system $\boldsymbol{M}$, $\boldsymbol{M}_0$ is the non-disturbance part, and $\boldsymbol{G}_0= \boldsymbol{M}_0(\boldsymbol{I}-\boldsymbol{M}_0)^{-1}$

$$G=G_0+\Delta G=(M_0+\Delta M)(I-M_0-\Delta M)^{-1} \quad (22)$$

Then we have the structural perturbation:

$$\Delta G = \frac{M_0 + \Delta M - G_0(I - M_0 - \Delta M)}{I - M_0 - \Delta M} \tag{23}$$

Therefore, the stability of the transfer alignment with H∞ filtering in Fig. 4 is equivalent to robust stability of the closed loop system in Fig. 7. Where, $\boldsymbol{M}=(\boldsymbol{I}+\boldsymbol{G})^{-1}\boldsymbol{G}$.

Let $\Delta = I + \frac{\Delta G}{G}$, and ΔG was obtained by ΔM :

$$M = M_0 + \Delta M = (\frac{1}{2}B_1 + I)(A + \Delta A) + \frac{1}{2}B_1 Y_\infty C_2^T C_2$$
$$= (\frac{1}{2}B_1 + I)A + \frac{1}{2}B_1 Y_\infty C_2^T C_2 + (\frac{1}{2}B_1 + I)\Delta A \tag{24}$$

So,

$$M_0 = (\frac{1}{2}B_1 + I)A + C = (\frac{1}{2}B_1 + I)A + \frac{1}{2}B_1 Y_\infty C_2^T C_2 \tag{25}$$

$$\Delta M = (\frac{1}{2}B_1 + I)\Delta A \tag{26}$$

According to the **robust stability theorem,** the infinite norm $\|\boldsymbol{\Delta}\|_\infty$ and the structured singular value $\mu_\Delta(\boldsymbol{G}_0)$ of the nominal system G_0 are then calculated to judge whether the items, namely, $\|\boldsymbol{\Delta}\|_\infty<1/\beta$ and $\mu_\Delta(\boldsymbol{G}_0)<\beta$ are satisfied at the same time, so as to evaluate the robust stability of the feedback system.

5 Equations and Mathematical Expressions

In this section, the mathematical simulations have been carried out to test the robust stability of the transfer alignment filter in the uniform motion, at the speed of 10m/s. The discrete filtering model of the transfer alignment can be expressed in Eq. (27), and the parameters setting are summarized in Tab. 1.

$$\begin{aligned}\boldsymbol{X}_k &= \boldsymbol{\phi}_{k,k-1}\boldsymbol{X}_{k-1} + \boldsymbol{\Gamma}_{k,k-1}\boldsymbol{W}_{k-1} \\ \boldsymbol{Z}_k &= \boldsymbol{H}_k\boldsymbol{X}_k + \boldsymbol{V}_k \\ \boldsymbol{Y}_k &= \boldsymbol{X}_k\end{aligned} \tag{27}$$

Where, $\boldsymbol{X}_k$ is the system state vector at time k, $\boldsymbol{\phi}_{k,k-1}$ is the state transition matrix, $\boldsymbol{\Gamma}_{k,k-1}$ is the system noise matrix, $\boldsymbol{W}_k$ is the system noise, $\boldsymbol{Z}_k$ is the measurement, $\boldsymbol{H}_k$ is the measurement matrix, $\boldsymbol{V}_k$ is the system measurement noise, $\boldsymbol{Y}_k$ is the output.

Table 1: parameters setting

Gyros' drift	0.1 °/h
Gyros' random	0.05 °/h
Accelerators' bias	1 mg
Accelerators' random	0.5 mg

The simulation is carried out in the North-East-Up (ENU) coordination system, and we simulated the velocity matching measurement for an illustration. The state vector is $\boldsymbol{X}_k$= [δV_e δV_n φ_e φ_n φ_u ∇_e ∇_n ε_e ε_n ε_u] and the measurement vector is consist of the northern velocity and eastern velocity $\boldsymbol{Z}_k$=[δV_e δV_n]. The system model is:

$$\phi_{k,k-1}=\begin{bmatrix} F & C \\ 0_{5x5} & 0_{5x5} \end{bmatrix}=\begin{bmatrix} F_{11} & F_{12} & 0 & -f_u & f_n & c_{11} & c_{12} & 0 & 0 & 0 \\ F_{21} & F_{22} & f_u & 0 & -f_e & c_{21} & c_{22} & 0 & 0 & 0 \\ 0 & -\frac{1}{R_n} & 0 & F_{34} & F_{35} & 0 & 0 & c_{11} & c_{12} & c_{13} \\ \frac{1}{R_e} & 0 & F_{43} & 0 & -\frac{V_n}{R_n} & 0 & 0 & c_{21} & c_{22} & c_{23} \\ \frac{tgL}{R_e} & 0 & F_{53} & \frac{V_n}{R_n} & 0 & 0 & 0 & c_{31} & c_{32} & c_{33} \\ 0 & 0 & 0 & 0 & 0 & 0 & 0 & 0 & 0 & 0 \\ 0 & 0 & 0 & 0 & 0 & 0 & 0 & 0 & 0 & 0 \\ 0 & 0 & 0 & 0 & 0 & 0 & 0 & 0 & 0 & 0 \\ 0 & 0 & 0 & 0 & 0 & 0 & 0 & 0 & 0 & 0 \\ 0 & 0 & 0 & 0 & 0 & 0 & 0 & 0 & 0 & 0 \end{bmatrix} \tag{28}$$

Where, c_{ij} (i,j=1,2,3) is the element of the attitude matrix, and $F_{11}=\frac{V_n}{R_n}tgL-\frac{V_u}{R_e}$, $F_{34}=\omega_{ie}\sin L+\frac{V_e}{R_e}tgL$ $F_{35}=-(\omega_{ie}\cos L+\frac{V_e}{R_e})$, $F_{43}=-F_{34}$, $F_{53}=-F_{35}$

Considering the system structure perturbation caused by the dynamic influence, we have assigned different uncertainties with several parameters in the system matrix: F_{11}(±10%), F_{12}(±2%) and F_{22}(±4%). As it is seen that, the uncertain parameters mainly cover velocity-relative factors, they are two element of the principal diagonal, one element with velocity and one element with position. Then, the bode diagrams in Fig. 8-Fig. 10 are of help to analyze the robustness stability of the transfer alignment system.

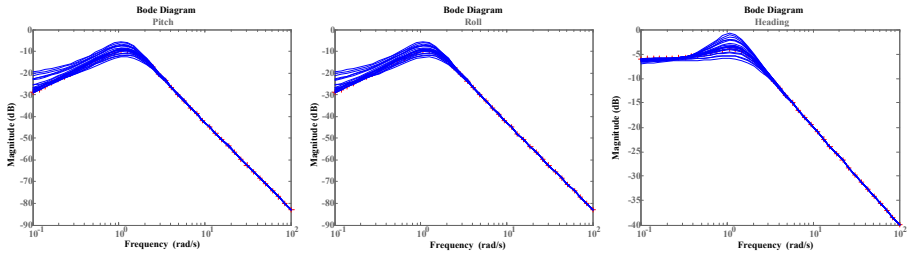

Figure 8: Frequency response of the attitudes

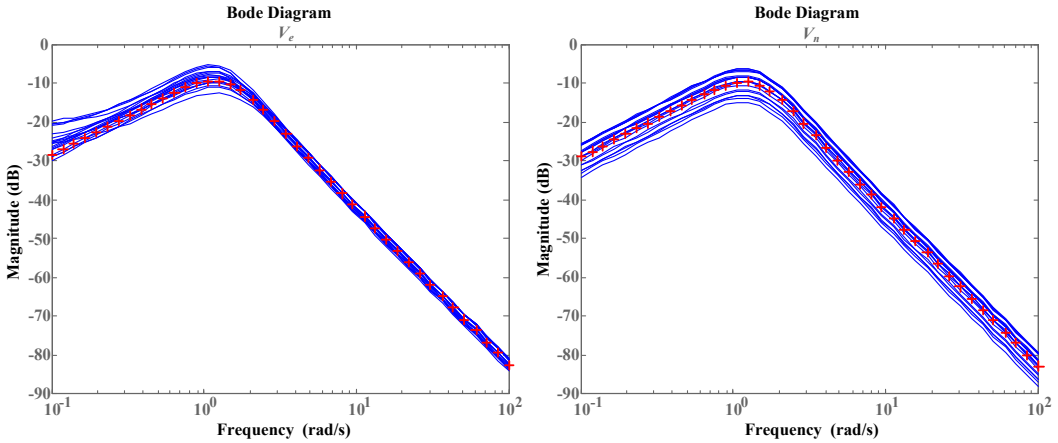

Figure 9: Frequency response of then northern and western velocities

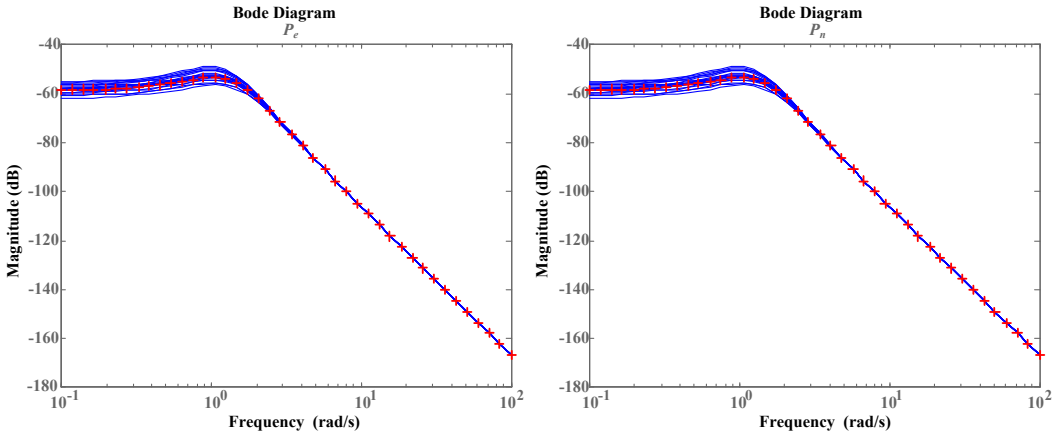

Figure 10: Frequency response of the northern and western positions

In these figures, due to the uncertainty of the system, the frequency response of the plant is different from the nominal model. The red "+" indicates the nominal model and the

blue dashed line indicates the results of 20 random samples for the model with uncertainty. Obviously, the uncertainty of the model changes the frequency response curve of the system. Because of the correlation and coupling of system parameters, the velocity uncertainties result in disturbances in the output of the alignment. It can be clearly seen that the perturbation on the attitudes are more serious, which easily lead to the operating frequency band. The positions are less perturbed by the uncertainties.

6 Concluding remarks

An algorithm of robustness stability analysis has been proposed for the transfer alignment to evaluate the impact of uncertainty on the navigation system. Based on the theory of the structured singular value analysis, a feedback structure of the transfer alignment filtering system has been developed, where the H∞ filter is adopted to perform the process. Furthermore, simulations have been carried out to exemplify the use of the proposed algorithm. The significance of this research is to find a way to evaluate the performance of the transfer alignment process when the system incorporates structural uncertainties under complex dynamic conditions, so as to further guide and improve the system design. This paper preliminarily validates the proposed algorithm, while different conditions like the vehicle maneuver motion, time delay, vibration and swaying environment that could introduce system uncertainties need elaborated robustness stability analysis. Such issue will be further addressed in the future study.

Acknowledgement: This work is supported by National Natural Science Foundation of China, No. 61803203, and the Fundamental Research Funds for the Central Universities, No. 30918011305.

References

Bottura, C. P.; Neto, M. F. S. (2000): Robust speed control of an induction motor: an H_∞ control theory approach with field orientation and μ-analysis. *IEEE Transactions on Power Electronics*, vol.15, no.5, pp. 908-915.

Candès, E. J.; Romberg, J.; Tao, T. (2006): Robust uncertainty principles: Exact signal reconstruction from highly incomplete frequency information. *IEEE Transactions on Information Theory*, vol. 52, no. 2, pp. 489-509.

Doyle, J. C. (1985): Structured uncertainty in control system design. *24th IEEE Conference on Decision and Control*, vol. 24, pp. 260-265.

He, Y.; Wu, M.; She, J. H.; Liu, G. P. (2004): Delay-dependent robust stability criteria for uncertain neutral systems with mixed delays. *Systems & Control Letters*, vol. 51, no. 1, pp. 57-65.

Kim, J.; Cho, K. H. (2016): Robustness analysis of network modularity. *IEEE Transactions on Control of Network Systems*, vol. 3, no. 4, pp. 348-357.

Li, H.; Chen, B.; Zhou, Q.; Qian, W. (2009): Robust stability for uncertain delayed fuzzy Hopfield neural networks with Markovian jumping parameters. *IEEE Transactions on Systems, Man, and Cybernetics, Part B* (*Cybernetics*), vol. 39, no. 1, pp. 94-102.

Liu, Y.; Wang, Z.; He, X.; Zhou, D. H. (2017): Finite-horizon quantized H∞ filter design for a class of time-varying systems under event-triggered transmissions. *Systems & Control Letters*, vol. 103, pp. 38-44.

Liu, J.; Zhang, W.; Rizzoni, G. (2018): Robust stability analysis of dc microgrids with constant power loads. *IEEE Transactions on Power Systems*, vol. 33, no. 1, pp. 851-860.

Packard, A.; Doyle, J. (1993): The complex structured singular value. *Automatica*, vol. 29, no. 1, pp. 71-109.

Pavel, L. (2004): A μ-analysis application to stability of optical networks. *Proceedings of the American Control Conference*, no. 5, pp. 3956-3961.

Wang, X. L.; Yang, G. H. (2018): Robust H∞ filter design for discrete-time interconnected fuzzy systems with partially unknown membership functions and past output measurements. *Neurocomputing*.

Yang, G. H.; Che, W. W. (2008): Non-fragile H∞ filter design for linear continuous-time systems. *Automatica*, vol. 44, no. 11, pp. 2849-2856.

Zhao, J. (2018): Dynamic state estimation with model uncertainties using H∞ extended Kalman filter. *IEEE Transactions on Power Systems*, vol. 33, no. 1, pp. 1099-1100.

Zhao, L.; Qiu, H.; Feng, Y. (2016): Analysis of a robust Kalman filter in loosely coupled GPS/INS navigation system. *Measurement*, no. 80, pp. 138-147.

Zhou, K.; Doyle, J. C.; Glover, K. (1996): *Robust and Optimal Control*, vol. 40, pp. 146. New Jersey, Prentice Hall.

Zhou, T.; Lian, B.; Yang, S.; Zhang, Y.; Liu, Y. (2018): Improved GNSS cooperation positioning algorithm for indoor localization. *Computers, Materials & Continua*, vol. 56, no. 2, pp. 225-245.